engineering proceedings

MDPI

Proceeding Paper

Flatfoot Detection in an Indian Population: Validation of Morphological Indices Using a Diagnostic Device †

Ketan Kalghatgi [1], Khyati Verma [1,*] and Bishwaranjan Das [2]

[1] Department of Mechanical Engineering, National Institute of Technology Surathkal, Mangaluru 575025, Karnataka, India; kalghatgiketan@gmail.com
[2] KMC Hospital, Dr. B.R. Ambedkar Circle, Mangalore 575001, Karnataka, India; bishwaranjan0312@gmail.com
* Correspondence: kverma@nitk.edu.in
† Presented at the 4th International Conference on Future Technologies in Manufacturing, Automation, Design and Energy 2024 (ICOFT 2024), Karaikal, India, 12–13 November 2024.

Abstract: Flatfoot, or pes planus, is a condition where the foot's arch collapses, leading to complications such as pain, gait abnormalities, and an increased risk of injury. Accurate and early diagnosis is critical for effective treatment. Traditional diagnostic methods, including radiographic imaging, footprint analysis, and plantar pressure measurement, often require specialized equipment and are subjective. This study proposes a novel diagnostic device that captures 2D plantar foot images to calculate key morphological indices, including the Staheli Index, Clark's Angle, and Chippaux–Smirak Index, for flatfoot detection. The device, designed with off-the-shelf components, includes a transparent toughened glass platform and LED illumination to capture images using web cameras. A Python-based application was developed for image acquisition, segmentation, and stitching. The device was tested on 55 participants aged 18–28, and the extracted morphological indices were validated against established thresholds for flatfoot diagnosis. The results showed that the Staheli Index, Chippaux–Smirak Index, and Clark's Angle reliably detected flatfoot in participants. The study highlights the potential of this device for non-invasive, accurate, and rapid flatfoot diagnosis. Future advancements in deep learning could enhance its capabilities, making it a valuable tool for proactive healthcare in foot deformity detection.

Keywords: flatfoot detection; planter image analysis; foot morphological studies

check for updates

Academic Editors: Karpagaraj Anbalagan and Sendhil Kumar Natarajan

Published: 3 June 2025

Citation: Kalghatgi, K.; Verma, K.; Das, B. Flatfoot Detection in an Indian Population: Validation of Morphological Indices Using a Diagnostic Device. *Eng. Proc.* **2025**, *95*, 6. https://doi.org/10.3390/engproc2025095006

Copyright: © 2025 by the authors. Licensee MDPI, Basel, Switzerland. This article is an open access article distributed under the terms and conditions of the Creative Commons Attribution (CC BY) license (https://creativecommons.org/licenses/by/4.0/).

1. Introduction

The collapse of the medial longitudinal arch is a characteristic of flatfoot (pes planus), a condition that can cause musculoskeletal problems and change gait mechanics. To avoid long-term problems, an accurate diagnosis is essential. Plantar pressure measurement, footprint analysis, and radiographic imaging are examples of traditional techniques [1,2]. These methods are limited in their applicability in standard clinical practice, though, because they either entail radiation exposure, call for specialized equipment, or depend on subjective evaluation [3].

For the objective and non-invasive evaluation of flatfoot, morphological indices offer a substitute. It is common practice to assess foot arch structure using the Staheli Index, Chippaux–Smirak Index, and Clarke's Angle. The study found that flatfoot is indicated by foot parameters such as a Staheli Index above 0.8125 and a Chippaux–Smirak Index above 0.4, while arch collapse is suggested by a Clarke's Angle below 37.5 degrees [4]. Despite being validated in a variety of populations, these indices need threshold values that are specific to a given region in order to improve diagnostic accuracy [5].

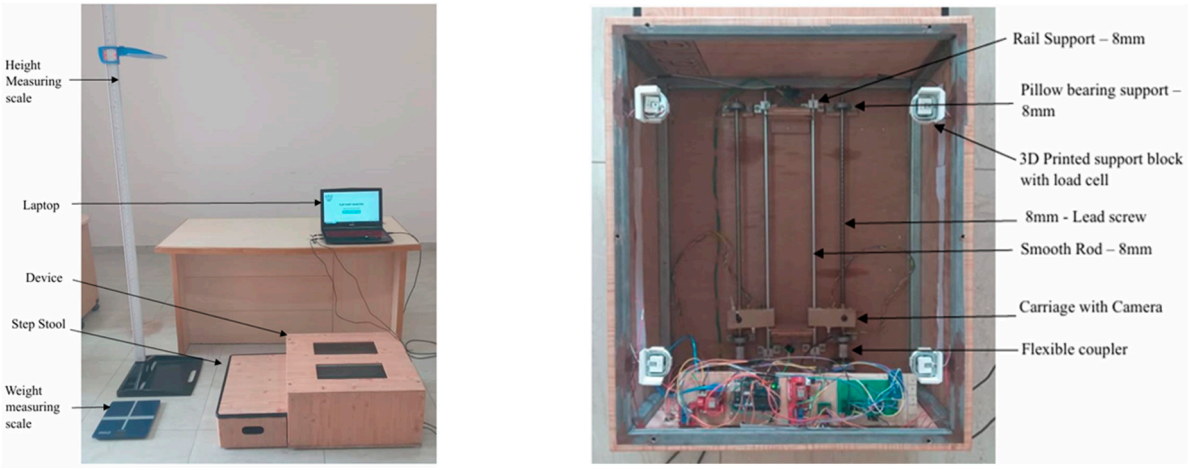
Automated diagnostic tools are crucial for improving reproducibility and reliability, according to recent studies. Plantar pressure distribution analysis has been shown to be an effective way to distinguish between different types of flatfoot [6,7], has emphasized the importance of radiographic parameters like the talar uncoverage angle in diagnosing adult-acquired flatfoot. Furthermore, research has demonstrated that personalized foot orthoses considerably enhance patient-reported results, bolstering the necessity of precise detection [8].

Despite these developments, little is known about the Indian population's use of diagnostic tools to validate morphological indices. By creating a specially designed plantar foot imaging system that extracts morphological parameters for objective and repeatable flatfoot detection, this study fills this gap.

2. Materials and Methods

2.1. Device Design and Setup

The diagnostic device for capturing 2D plantar foot images was developed using off-the-shelf components. It features a metal frame platform with a transparent toughened glass surface capable of supporting up to 150 kg, enclosed by plywood panels. Uniform illumination is provided by LED lights along the glass edges and inside the platform, with foot placement cutouts to reduce ambient light interference. The imaging system includes two Logitech C270 digital cameras (720 p/30 fps, 0.9 MP, 55° FOV) manufactured by Logitech Asia Pacific Ltd, Hong Kong, China are mounted beneath the glass on a motorized linear sliding mechanism as shown in Figure 1. A Python v3.9-based desktop application controls the device and collects data, while a step stool, height, and weight scales are included for accessibility and additional measurements. Figure 1 shows the complete setup of the system.



(**a**) (**b**)

Figure 1. (**a**) Complete setup of the system.; (**b**) imaging system used for the device.

2.2. Image Acquisition

The image acquisition process captures high-contrast, segmented plantar foot images using Total Internal Reflection (TIR)-based illumination, controlled imaging, and automated stitching. Subjects stand barefoot on a transparent toughened glass plate, with green LED strips along the edges highlighting foot contact areas via TIR. Two Logitech C270 cameras, mounted on a motorized linear carriage, move along the foot to cpture images, with a stepper motor ensuring stable motion and full coverage.

Effect of Lighting and Skin Tone: The enclosed design prevents ambient light interference, ensuring consistent imaging. TIR-based illumination makes the process independent of skin tone variations.

Image Stitching and Pre-processing: The pre-processing steps include resizing and making the image smooth for feature detection and matching. Figure 2 shows a block diagram of the various steps involved in image processing and stitching.

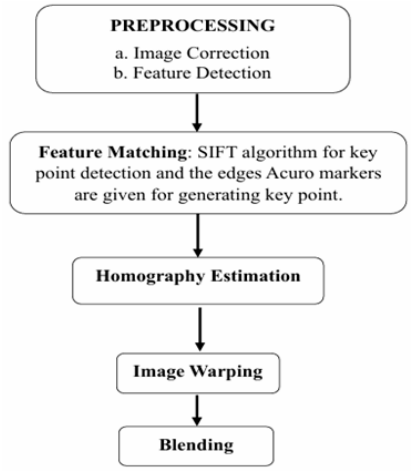


Figure 2. Block diagram representing the pre-processing steps and image stitching.

- Feature Detection and Matching: The SIFT algorithm identifies and matches key features across overlapping images.
- ArUco Marker Integration: Markers along the glass edges provide reference points for alignment, eliminating reliance on foot-specific markers.
- Homography Estimation and Image Warping: A transformation model aligns images based on detected key points for geometric consistency.
- Blending and Seamless Integration: Overlapping regions are merged using blending algorithms to create a high-resolution, distortion-free composite image.
- Segmentation and Background Removal: Color-based segmentation isolates the foot region, with a custom tuning interface for adjustments. The final image features a black background for easy feature extraction as shown in Figure 3.



(**a**) (**b**) (**c**)

Figure 3. (**a**) Captured stitched image of the plantar side of the foot from the device; (**b**) image after segmentation with index values marked on the foot image; (**c**) dialog box showing options to tune the segmentation process.

2.3. Measurement of Morphological Parameters

Key anatomical landmarks are identified on the segmented foot image, and morphological indices are calculated:

- Foot Length and Width: Determined by detecting the outermost foot boundaries.
- Clark's Angle, Heel, and Forefoot Angles: Measured using key points along the plantar surface. These indices are visualized directly on the segmented image.

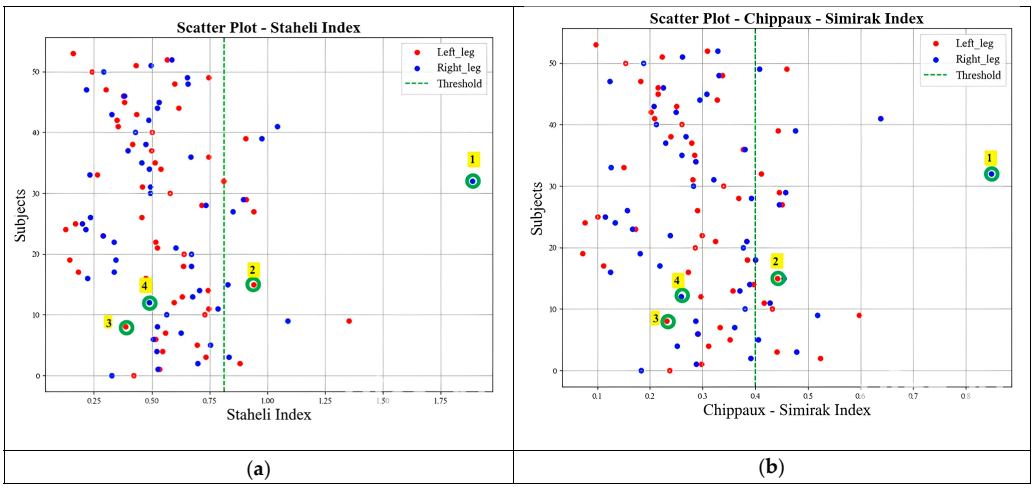
3. Results and Discussion

A total of 55 participants were tested to validate the system. Each provided basic information (height, weight, shoe size, and foot conditions), Figure 4 shows the subject undergoing foot scanning process. The collected data were analyzed using scatter plots for three morphological indices: Staheli Index, Chippaux–Simirak Index, and Clarke's Angle. The reference values for these indices were taken from previous studies.



Figure 4. Subject undergoing foot scanning.

- Staheli Index: As shown in Figure 5a, most participants' index values were below the reference limit of 0.8125, suggesting a normal foot arch structure. However, some deviations were observed in participants suspected of having flatfeet.
- Chippaux–Simirak Index: Figure 5b shows a scatter plot with a reference threshold of 0.4 for flatfoot detection. Most participants had values below this limit, indicating normal foot morphology.



(**a**) (**b**)

Figure 5. (**a**) Scatter plot of Staheli Index with (1–4) being highlighted subjects compared in Table 1; (**b**) Scatter plot of Chippaux–Simirak Index with (1–4) being highlighted subjects compared in Table 1.

- Clarke's Angle: The scatter plot in Figure 6 demonstrates that most participants had Clarke's angles above 37.5 degrees, which is considered normal. However, a few participants showed significantly lower values, suggesting potential flatfoot conditions.

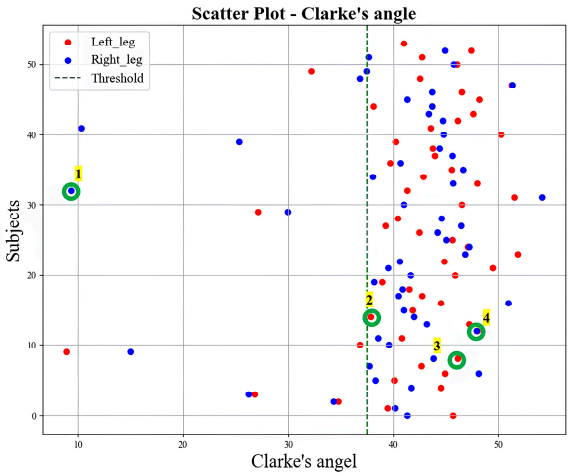


Figure 6. Scatter plot of Clarke's Angle with (1–4) being highlighted subjects compared in Table 1.

Table 1 summarizes the index values for selected subjects, revealing notable deviations in participants with flatfeet, which reinforces the reliability of these indices for diagnosing flatfoot conditions.

Table 1. Index and angle values for subjects with flatfoot and normal foot conditions.

Subject	Condition	Chippaux–Simirak Index	Clark Angle	Staheli Index
Reference		0.4	37.5 º	0.8125
1	Flatfoot	0.848	9.3 º	1.887
2	Flatfoot	0.442	37.8 º	0.942
3	Normal foot	0.232	46.1 º	0.387
4	Normal foot	0.428	38.5 º	0.48

º—is a degree notation.

A 2D plantar foot imaging system was successfully created in this study, and a desktop application was integrated for effective data collection and analysis. When evaluating foot morphology using recognized indices like the Chippaux–Simirak, Staheli, and Clarke's indices, the system showed an excellent accuracy. The accuracy of image stitching was greatly improved by the use of ArUco markers, guaranteeing the results' resilience and repeatability. These results demonstrate the system's potential for precise and non-invasive flatfoot diagnosis. Incorporating deep learning models for automated diagnosis and field-use device optimization, with an emphasis on ergonomic design and portability improvements, are future research directions. With these developments, this technology may become a useful tool for proactive healthcare in the detection of foot deformities, providing an affordable and easily accessible option for early diagnosis and treatment planning.

In comparison to other diagnostic methods, such as the medical imaging techniques used for plantar heel pain, our approach focuses on non-invasive morphological assessments rather than requiring specialized imaging like ultrasound or MRI [9]. While medical imaging can provide detailed insights into conditions such as plantar fasciopathy [10], our system offers a more accessible and cost-effective solution for initial screenings. The use of morphological indices in our study is consistent with the broader literature on foot conditions. For instance, studies on plantar vein thrombosis emphasize the importance of imaging techniques like ultrasound and MRI for diagnosing venous disorders in the

foot [11]. Similarly, MRI has been shown to be effective in diagnosing metatarsophalangeal plantar plate tears, highlighting the role of imaging in detailed assessments of foot anatomy [12]. However, our system's reliance on morphological indices provides a unique advantage in terms of simplicity and portability, making it suitable for field use in settings with limited medical facilities. Future enhancements could include integrating deep learning models for automated diagnosis and optimizing the device for real-time feedback, which would further enhance its utility in clinical settings.

4. Conclusions

A 2D plantar foot imaging system was successfully created in this study, and a desktop application was integrated into the system for effective data collection and analysis. When evaluating foot morphology using recognized indices like the Chippaux–Simirak, Staheli, and Clarke's indices, the system showed excellent accuracy. The accuracy of image stitching was greatly improved by the use of ArUco markers, guaranteeing the results' resilience and repeatability. These results demonstrate the system's potential for precise and non-invasive flatfoot diagnosis. Incorporating deep learning models for automated diagnosis and field-use device optimization, with an emphasis on ergonomic design and portability improvements, are future research directions. With these developments, this technology may become a useful tool for proactive healthcare in the detection of foot deformities, providing an affordable and easily accessible option for early diagnosis and treatment planning.

5. Limitations

There are multiple limitations to this study. First off, a deep learning model cannot be developed with the 55-person dataset; further improvements will require a larger and more varied sample. The scanning procedure, which takes around a minute, might also be too long for patients who have trouble balancing. Because dust, moisture, or dirt can impair segmentation accuracy, the need for a clean glass surface and dry feet to guarantee optimal image capture presents practical difficulties. The integration of deep learning algorithms would be necessary to achieve a real-time flatfoot diagnosis, which is currently not possible with the current setup, even though the current system offers accurate assessments.

Author Contributions: Conceptualization, K.V.; methodology, K.K.; software, K.K.; validation, K.K. and K.V.; formal analysis, B.D.; investigation, K.K.; resources, K.V.; data curation, K.K.; writing—original draft preparation, K.K.; writing—review and editing, K.V.; visualization, K.K.; supervision, K.V. All authors have read and agreed to the published version of the manuscript.

Funding: This research received no external funding.

Institutional Review Board Statement: Approval obtained from Institutional Ethics Committee-Kasturba Medical College, Mangalore (Approval No: IEC KMC MLR 09/2021/292).

Informed Consent Statement: Informed consent was obtained from all subjects involved in the study.

Data Availability Statement: Data for this study are available upon request from the corresponding author.

Conflicts of Interest: Author Bishwaranjan Das was employed by the KMC Hospital. The remaining authors declare that the research was conducted in the absence of any commercial or financial relationships that could be construed as a potential conflict of interest.

References

1. Harris, E.J.; Vanore, J.V.; Thomas, J.L.; Kravitz, S.R.; Mendelson, S.A.; Mendicino, R.W.; Gassen, S.C. Diagnosis and treatment of pediatric flatfoot. *J. Foot Ankle Surg.* **2004**, *43*, 341–373. [CrossRef] [PubMed]
2. Roth, S.; Roth, A.; Jotanovic, Z.; Dembic, Z. Navicular index for differentiation of flatfoot from normal foot. *Int. Orthop.* **2013**, *37*, 1107–1112. [CrossRef] [PubMed]
3. Pauk, J.; Daunoraviciene, K.; Ihnatouski, M.; Griskevicius, J.; Raso, J.V. Analysis of the plantar pressure distribution in children with foot deformities. *Acta Bioeng. Biomech.* **2010**, *12*, 29–34. [PubMed]
4. Koirala, S.; Khanal, G.P.; Shah, S.; Khanal, L.; Yadav, P.; Baral, P. Calculation of Staheli's Plantar Arch Index, Chippaux-Smirak Index, Clarke's Angle Prevalence and Predictors of Flat Foot: A cross-sectional study. *Austin J. Anat.* **2021**, *8*, 1095.
5. Ramos, A.; Fernandes, S.; Pooja, P.; Panicker, P.J.; Krishnan, P. Assessment of flat foot using plantar arch index in young adults. *Biomedicine* **2021**, *41*, 535–538. [CrossRef]
6. Khan, F.; Chevidikunnan, M.F.; BinMulayh, E.A. Plantar pressure distribution in the evaluation and differentiation of flatfeet. *Gait Posture* **2023**, *101*, 82–89. [CrossRef] [PubMed]
7. Krishnaprasad, P.R.; Gowtham, Y.; Shah, H. Comparison of Radiological Parameters to Predict Adult Acquired Flatfoot in the Indian Population. *Muscles Ligaments Tendons J.* **2024**, *14*, 301–305. [CrossRef]
8. Oerlemans, L.N.T.; Peeters, C.M.M.; Munnik-Hagewoud, R. Foot orthoses for flexible flatfeet: A systematic review and meta-analysis. *BMC Musculoskelet. Disord.* **2023**, *24*, 16. [CrossRef] [PubMed]
9. Drake, C.; Whittaker, G.A.; Kaminiski, M.R.; Chen, J.; Keenan, A.M.; Rathleff, M.S.; Robinson, P.; Landorf, K.B. Medical imaging for plantar heel pain: A systematic review and meta-analysis. *J. Foot Ankle Res.* **2022**, *15*, 4. [CrossRef] [PubMed]
10. McNally, E.G.; Shetty, S. Plantar Fascia: Imaging Diagnosis and Guided Treatment. *Semin. Musculoskelet. Radiol.* **2010**, *14*, 334–343. [CrossRef] [PubMed]
11. Miranda, F.C.; Castro, A.A.; Yosshimura, F.B.; Godoy Santos, A.L.; Barrows Santos, C.; Rosemberg, L.A.; Taneja, A.K. Imaging Features of Plantar Vein Thrombosis: An Easily Overlooked Condition in the Differential Diagnosis of Foot Pain. *Diagnostics* **2024**, *14*, 126. [CrossRef] [PubMed]
12. Yamada, A.F.; Crema, M.D.; Nery, C.; Baumfeld, D.; Mann, T.S.; Skaf, A.Y.; Fernandes, A.C.R. Second and Third Metatarsophalangeal Plantar Plate Tears: Diagnostic Performance of Direct and Indirect MRI Features Using Surgical Findings as the Reference Standard. *Musculoskelet. Imaging* **2017**, *209*, 101–108. [CrossRef] [PubMed]

Disclaimer/Publisher's Note: The statements, opinions and data contained in all publications are solely those of the individual author(s) and contributor(s) and not of MDPI and/or the editor(s). MDPI and/or the editor(s) disclaim responsibility for any injury to people or property resulting from any ideas, methods, instructions or products referred to in the content.